Structural, Magnetic and Electrical Properties of the Ternary Silicide $Gd_6Co_{1.67}Si_3$ Derived from the Hexagonal $Ho_4Co_{3.07}$ (or $Ho_6Co_{4.61}$) Type Structure

Etienne Gaudin[a], François Weill[a,b], and Bernard Chevalier[a]

[a] Institut de Chimie de la Matière Condensée de Bordeaux (ICMCB), CNRS [UPR 9048], Université Bordeaux 1, Avenue du Docteur A. Schweitzer, F-33608 Pessac Cedex, France
[b] Centre de Ressource en Microscopie Electronique et Microanalyse, CREMEM, Université Bordeaux 1, 350 Cours de la Libération, F-33400 Talence Cedex, France

Reprint requests to Dr. B. Chevalier. E-mail: chevalie@icmcb-bordeaux.cnrs.fr

Z. Naturforsch. **61b,** 825 – 832 (2006); received February 23, 2006

Dedicated to Professor Wolfgang Jeitschko on the occasion of his 70th birthday

The title compound was discovered as an impurity phase in many GdCoSi samples. It crystallizes in the hexagonal space group $P6_3/m$ with $a = 11.7787(5)$ and $c = 4.1640(2)$ Å. Using X-ray powder diffraction, an ordered distribution between Co and Si was found but one site is not fully occupied by Co for steric reasons. Magnetization measurements reveal that $Gd_6Co_{1.67}Si_3$ exhibits a ferromagnetic transition at $T_C = 294(2)$ K, a Curie temperature similar to that reported for pure gadolinium. This magnetic ordering has been confirmed by electrical resistivity investigations.

Key words: Rare-Earth Intermetallics, Electron Microscopy, Crystal Chemistry of Intermetallics, Magnetic Properties, Electrical Resistance

Introduction

Recently, we have shown that the ternary compounds CeCoSi and CeCoGe which crystallize in the tetragonal CeFeSi-type structure absorb hydrogen at 523 K [1 – 3]. This H-insertion modifies greatly their magnetic properties. For instance, interesting antiferromagnetic → spin fluctuation behaviour was found upon the hydrogenation of CeCoSi [2, 3].

In order to extend our study on the influence of hydrogenation on the magnetic properties of the *RE*CoSi compounds (*RE* = rare earth), we have prepared several samples of GdCoSi. This ternary silicide exhibits an antiferromagnetic ordering of the gadolinium substructure at $T_N = 175(3)$ K (*standard deviation of the least-significant digit is given in parentheses throughout the paper*) [4]. The magnetization measurements performed on various GdCoSi samples have revealed for some of them (inset of Fig. 1) the presence of two magnetic transitions: (i) one at 169(2) K in agreement with the antiferromagnetic character of GdCoSi, and (ii) a second one close to 295(2) K showing a ferromagnetic behaviour. A similar result was reported previously [5]; the two transitions were considered as in-

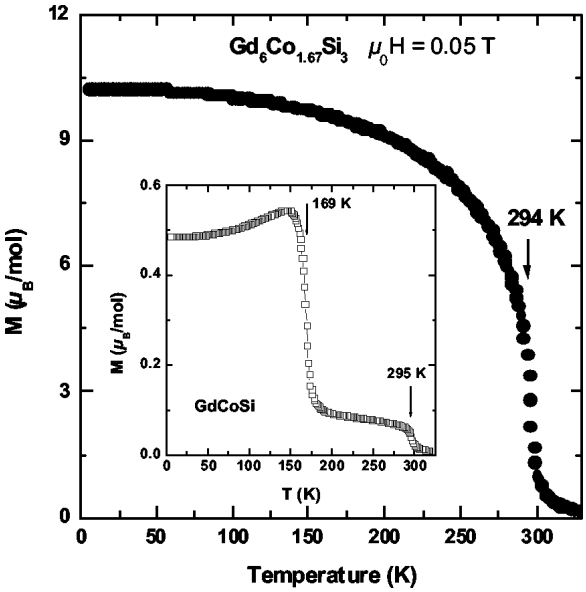

Fig. 1. Temperature dependence of the magnetization, measured with an applied field μ_0H = 0.05 T, of $Gd_6Co_{1.67}Si_3$ and GdCoSi (inset).

trinsic, the high-temperature anomaly being linked to the magnetic ordering of the cobalt substructure. But the analysis of our GdCoSi samples by microprobe has suggested that this last transition is connected to the presence of some amounts of an impurity phase: the ternary silicide $Gd_6Co_{1.67}Si_3$.

In this paper, we present and discuss the structural, magnetic and electrical properties of $Gd_6Co_{1.67}Si_3$. The existence of this ternary silicide was not reported in the recent paper devoted to the phase equilibria in the Gd-Co-Si system at 773 K [6]. On the contrary, Morozkin *et al.* claim the existence of $Gd_6Co_3Si_2$ prepared by an arc-melting process without annealing [7]. This last ternary compound, which crystallizes in the hexagonal $Ce_6Ni_2Si_3$-type structure, could be in equilibrium with $Gd_6Co_{1.67}Si_3$.

Experimental Section

A polycrystalline $Gd_6Co_{1.67}Si_3$ sample was synthesized by arc-melting a stoichiometric mixture of the pure elements (purity above 99.9%) in a high purity argon atmosphere. Then, the sample was turned over and remelted several times to ensure homogeneity. The weight loss during the arc-melting process was less than 0.5 wt%. Annealing was done for one month at 1073 K by enclosing the sample in an evacuated quartz tube. No attack of the quartz tube by the sample and *vice versa* was observed.

The composition as well as the homogeneity of the annealed sample are checked by microprobe analysis using a Cameca SX-100 instrument. The analysis was performed on the basis of intensity measurements of Gd-$L_{\alpha 1}$, Co-$K_{\alpha 1}$ and Si-$K_{\alpha 1}$ X-ray emission lines, which were compared with those obtained for $GdCo_2Si_2$ used as reference compound. The sample presents a perfect chemical homogeneity. The experimental atomic percentages Gd 56.4(2)%, Co 15.3(2)% and Si 28.3(2)% are close to those calculated for the $Gd_6Co_{1.67}Si_3$ composition (Gd 56.2%, Co 15.7% and Si 28.1%).

The electron diffraction investigation was carried out on a JEOL 2000FX microscope, operating at 200 kV, equipped with a double tilt specimen stage. Prior to the observation, the annealed sample was crushed in an agate mortar with alcohol. A drop of the suspension was deposited on a lacey carbon supported grid.

Unfortunately, the poor quality of the single crystals isolated from a crushed annealed $Gd_6Co_{1.67}Si_3$ sample, did not allow their use for crystal structure determination. X-ray powder diffraction data were collected with a Philips X-Pert diffractometer operating at room temperature and using Cu-K_α radiations. The powder diffraction pattern was scanned over the angular range $5-120^\circ$ with a step size of $\Delta(2\theta) = 0.02^\circ$. Rietveld refinement was performed using the Jana2000 program package [8]. The initial lattice parameters were taken from the electron diffraction study. The background was estimated by a Legendre polynom and the peak shape was described by a Lorentz function varying two profile coefficients. The refinement of peak asymmetry was performed using the Simpson parameter in Jana2000 [8]. Details of the refinements are gathered in

Table 1. Powder X-ray data collection and refinement parameters.

Temperature [K]	293
Wavelengths [Å]	1.54051 and 1.54433
Diffractometer	Philips X-Pert
2θ (°) Range	5 – 120
Step (°2θ); time per step (s)	0.02, 50
Crystal data	
Chemical formula	$Gd_6Co_{1.67}Si_3$
Space group	$P6_3/m$
Cell parameters [Å]	$a = 11.7787(5)$
	$c = 4.1640(2)$
Cell volume [Å^3]	500.31(4)
Z	2
D_x calculated [g cm^{-3}]	7.47
Refinement	
Structure refinement program	Jana2000
Profile function	Lorentz
Profile parameters	X = 2.7(4), Y = 15.0(10), Asym† = 2.6(3)
Background function	Legendre
No. of background parameters	12
Full No. of reflections	286
Full No. of refined parameters	12
R	0.0429
wR	0.0364
Rp	0.1241
R_{wp}	0.1611
χ^2	1.56

† Simpson asymetric parameter.

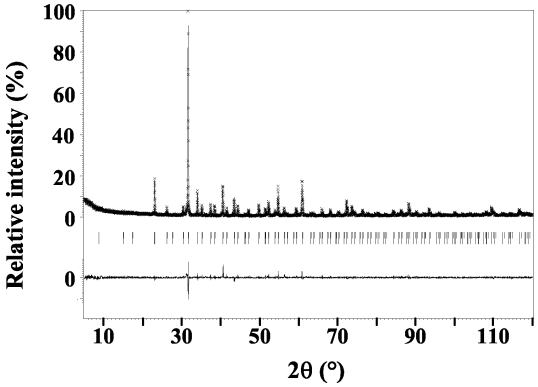

Fig. 2. Final profile refinement for $Gd_6Co_{1.67}Si_3$: observed (cross), calculated (full line), and difference (bottom) profiles. Reflection positions are indicated by tick marks.

	Atom	Site	*x*	*y*	*z*	B_{iso}	Occ.
Intermediate model	Gd1	6*h*	0.7630(7)	−0.0076(11)	1/4	0.37(13)	1
	Gd2	6*h*	0.1402(6)	0.5185(7)	1/4	0.38(11)	1
	Co1a	4*e*	0	0	0.09(2)	0.5†	0.32(5)
	Co1b	2*a*	0	0	1/4	0.5†	0.11(9)
	Co2	2*d*	2/3	1/3	1/4	0.1(9)	1.04(8)
	Si	6*h*	0.440(3)	0.163(4)	1/4	1.6(9)	1.08(6)
Final model	Gd1	6*h*	0.7627(6)	−0.0079(10)	1/4	0.34(12)	1
	Gd2	6*h*	0.1399(6)	0.5184(7)	1/4	0.38(11)	1
	Co1a	4*e*	0	0	0.088(15)	0.5†	0.30(5)‡
	Co1b	2*a*	0	0	1/4	0.5†	0.06(9)‡
	Co2	2*d*	2/3	1/3	1/4	0.5†	1
	Si	6*h*	0.439(3)	0.161(3)	1/4	0.5(5)	1

Table 2a. Atomic coordinates and atomic displacement parameters for $Gd_6Co_{1.67}Si_3$ (space group $P6_3/m$).

† Fixed; ‡ the sum of occupancies of Co1a and Co1b positions have been constrained to fit the expected stoichiometry.

	Atom	Site	*x*	*y*	*z*	B_{eq}	Occ.
$La_6Ni_{1.54}Si_3$	La1	6*h*	0.75860(5)	−0.01056(5)	1/4	1.41(1)	0.999(2)
	La2	6*h*	0.13869(5)	0.52021(5)	1/4	0.90(1)	1.000(2)
	Ni1	4*e*	0	0	0.104(4)	0.9‡	0.094(4)
	Ni3	2*a*	0	0	1/4	0.9‡	0.355(6)
	Ni2	2*d*	2/3	1/3	1/4	1.08(3)	0.994(7)
	Si	6*h*	0.4453(2)	0.1639(2)	1/4	1.01(4)	0.984(8)
$Gd_6Co_3Si_2$	Gd1	6*h*	0.770(2)	0.002(3)	1/4		1
	Gd2	6*h*	0.133(2)	0.520(2)	1/4		1
	Co2	2*b*	0	0	0		1
	Si2	2*d*	2/3	1/3	1/4		1
	Co1	6*h*	0.438(7)	0.142(6)	1/4		0.667
	Si1	6*h*	0.438	0.142	1/4		0.333

Table 2b. Atomic coordinates and atomic displacement parameters for $La_6Ni_{1.54}Si_3$ [11]† and $Gd_6Co_3Si_2$ [7] (space group $P6_3/m$).

† The setting of atomic positions has been changed for comparison with other structures; ‡ fixed in the refinement.

Table 3. Selected interatomic distances (Å) in $Gd_6Co_{1.67}Si_3$.

Gd1	Co1b (×1)	2.749(15)		[Co1a (×1)	1.33(12)]
	Co1a (×2)	2.83(2)		[Co1b (×1)	1.42(8)]
	Si (×2)	2.99(2)		[Co1a (×2)	2.08(12)]
	Si (×1)	3.02(4)		Co1b (×1)	2.75(8)
	Co1a (×2)	3.09(4)		Co1a (×1)	2.83(12)
	Co1b (×2)	3.449(12)		Gd1 (×3)	2.83(2)
	Gd1 (×4)	3.449(13)		Gd1 (×3)	3.09(4)
	Gd2 (×2)	3.610(13)			
	Gd2 (×1)	3.944(11)	Co1b	[Co1a (×2)	0.67(8)]
	Gd2 (×1)	3.983(12)		[Co1a (×2)	1.42(8)]
	Gd1 (×2)	4.164		[Co1b (×2)	2.082]
				Gd1 (×3)	2.749(15)
Gd2	Co2 (×2)	2.932(5)		Co1a (×2)	2.75(8)
	Si (×2)	3.06(3)		Gd1 (×6)	3.449(12)
	Si (×2)	3.09(3)			
	Si (×1)	3.25(4)	Co2	Si (×3)	2.42(3)
	Gd2 (×2)	3.576(11)		Gd2 (×6)	2.932(5)
	Gd1 (×2)	3.610(13)			
	Gd2 (×2)	3.736(9)	Si	Co2 (×1)	2.42(3)
	Gd1 (×1)	3.944(11)		Gd1 (×2)	2.99(2)
	Gd1 (×1)	3.983(12)		Gd1 (×1)	3.02(4)
	Gd2 (×2)	4.164		Gd2 (×2)	3.06(3)
				Gd2 (×2)	3.09(3)
Co1a	[Co1b (×1)	0.67(8)]		Gd2 (×1)	3.25(4)
	[Co1a (×1)	0.75(12)]			

Distances listed in brakets involve partially occupied sites and do not need to occur.

Table 1 and a plot of the final refinement is presented in Fig. 2. Tables 2a and 3 summarize respectively the positional parameters and interatomic distances relative to this refinement.

Magnetization measurements were performed using a Superconducting Quantum Interference Device (SQUID) magnetometer in the temperature range 1.8 – 360 K and applied fields of up to 5 T.

Electrical resistivity was carried out above 4.2 K on a polycrystalline sample using standard d. c. four-probe measurements. Due to the presence of microcracks in the sample, the absolute value of ρ could not be determined accurately; for this reason, a reduced representation is chosen.

Results and Discussion

Structural properties

X-ray powder analysis performed on the $Gd_6Co_{1.67}Si_3$ sample obtained after melting has revealed the presence of some quantities of the hexagonal Gd_5Si_3 silicide [9] coexisting with the major ternary compound. After annealing, Gd_5Si_3 is not detected.

From the electron diffraction patterns realized with the annealed sample, the whole reciprocal space has been built. The symmetry appears to be hexagonal and the parameters were found to be around $a = 11.7$ and $c = 4.1$ Å. Fig. 3 presents the [001] zone axis pattern characteristic of the hexagonal symmetry. Further-

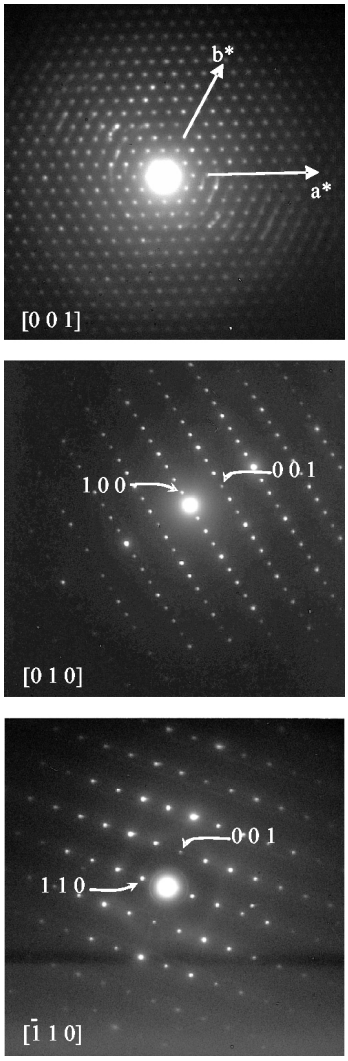

Fig. 3. Electron diffraction patterns of $Gd_6Co_{1.67}Si_3$ along the [0 0 1], [0 1 0] and [1 1 0] directions.

more, as no systematic reflection conditions have been detected in the [010] and [$\bar{1}$10] zone axis patterns, the presence of any glide plane can be excluded. It is worthwhile to note the absence of any diffuse scattering in the electron diffraction patterns indicating that the structure of this ternary compound has no default.

The chemical composition determined by microprobe analysis and the crystallographic properties of $Gd_6Co_{1.67}Si_3$ deduced from the electron diffraction investigation suggest that this ternary silicide adopts – like $Gd_4Co_{3.07}$ (or $Gd_6Co_{4.61}$) – the hexagonal $Ho_4Co_{3.07}$-type ($P6_3/m$ space group) [10]. Note that the condition (00l, l = 2*n*) related to the screw axis is

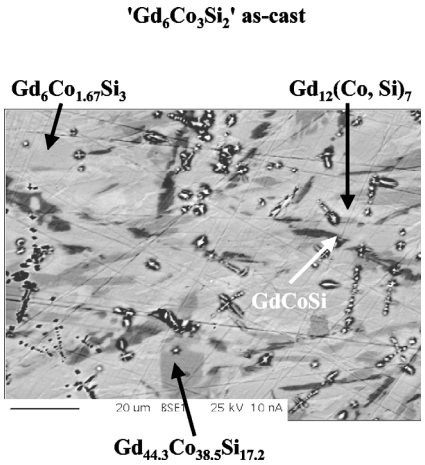

Fig. 4. Microstructure of a $Gd_6Co_3Si_2$ alloy obtained after melting and quenching. The various phases are indicated : $Gd_6Co_{1.67}Si_3$ (grey), $Gd_{12}(Co, Si)_7$ (light grey), $Gd_{44.3}Co_{38.5}Si_{17.2}$ (dark grey) and GdCoSi (black).

not observed in electron diffraction because of the double diffraction. The unit cell parameters of $Gd_6Co_{4.61}$ ($a = 11.591$ and $c = 4.054$ Å) are comparable to those determined for $Gd_6Co_{1.67}Si_3$ (Table 1). In this structure type, gadolinium occupies two crystallographic sites (6*h* and 6*h*) whereas cobalt is located on three sites (6*h*, 2*b* and 2*d*) but one of them (2*b*) is not fully occupied.

The unit cell parameters determined here for $Gd_6Co_{1.67}Si_3$ (Table 1) are similar to those reported by Morozkin *et al.* for $Gd_6Co_3Si_2$ ($a = 11.747(6)$ and $c = 4.163(1)$ Å) [7]. Nevertheless, our attempts to prepare this compound by arc melting followed by quenching as indicated in ref. [7] did not allow to obtain a single phase. Fig. 4 presents the characteristic microstructure, obtained by microprobe analysis (back-scattered image) of this as-cast sample. Four phases are clearly distinguished: (i) the major grey phase with the experimental atomic percentages Gd 56.7(4)%, Co 15.5(3)% and Si 27.7(3)% corresponding to $Gd_6Co_{1.67}Si_3$; (ii) the equiatomic compound GdCoSi (black) and two unknown intermetallics $Gd_{63.4}Co_{34.1}Si_{2.5}$ (or $Gd_{12}(Co, Si)_7$) (light grey) and $Gd_{44.3}Co_{38.5}Si_{17.2}$ (dark grey). This result confirms the non-existence of the compound $Gd_6Co_3Si_2$ and the absence of the solid solution $Gd_6(Co, Si)_{4.61}$. In other words, the new ternary silicide $Gd_6Co_{1.67}Si_3$ does not show a composition range.

The Rietveld refinement was started with the position of $Gd_6Co_{4.61}$ with the space group $P6_3/m$ [10]

(*i.e.*: Gd in two 6*h* positions and Co in 6*h*, 2*d* and 2*b*). After several attempts an ordering of cobalt and silicon atoms has been found, the former being located in the 2*b* and 2*d* positions and the latter in the 6*h* position. Nevertheless, the 2*b* position $(0,0,0)$ was not fully occupied by cobalt atoms and exhibited a high atomic displacement factor. Moreover the distance between two adjacent Co1 atoms, 2.08 Å, was too short ($r_{Co} = 1.252$ Å as metallic radius). This geometrical constraint has been previously noted by Lemaire *et al.* in the series $RE_6Co_{4.61}$ [10] and by Prots' *et al.* in similar ternary silicides $La_6Ni_{1.54}Si_3$ and $Nd_6Ni_{1.66}Si_3$ [11, 12]. After a Fourier analysis a splitting of the 2*b* Wyckoff position (in 4*e* position) has been introduced. The occupancy factor of the 4*e* position was found to be close to one third. The studies of homologous compounds by Prots' *et al.* [11, 12] on single-crystals have demonstrated the existence of a supplementary position 2*a* $(0,0,1/4)$ along the *c* direction. The partial occupancy of the 2*a* position has been tested in our refinement, and indeed a small amount of cobalt has been found in this site. In an intermediate model presented in the Table 2a, the refinement of occupancy factors of all positions, except gadolinium positions, was performed to prove the ordering between cobalt and silicon over the different Wyckoff positions. In the final model (Table 2a), the occupancy factors have been fixed to the ideal values and the sum of the occupancy values of the cobalt atoms in position $(0,0,z)$ has been fixed with respect to the stoichiometry. The atomic displacement parameters of Co1a and Co1b have been fixed to avoid correlation with refined occupancy parameters. This approach has been used by Prots' *et al.* [11] for the refinement of the structure of a $La_6Ni_{1.54}Si_3$ single-crystal. For the Co2 position in the last refinement the B_{iso} value was slightly negative with a strong standard deviation ($-0.1(7)$, to be compared with the value 0.1(9) of the intermediate model in Table 2a). Then the value was fixed to 0.5 and no significant changes in the fitted pattern and the reliability factors were observed.

Our refinement is not in agreement with the structural study of $Gd_6Co_3Si_2$ by Morozkin *et al.* (Table 2b) [7]. From our investigation it is clear that the ordering of cobalt and silicon over the different Wyckoff positions is not the same. Our attempts to use their model were not successful. For instance, if silicon replaces cobalt on the 2*d* positions (Co2 in our refinement), the refined occupancy is close to 200%.

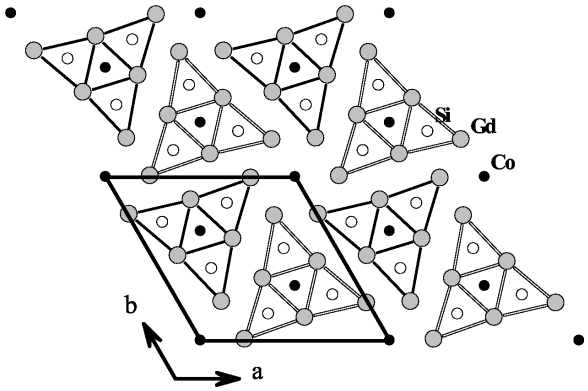

Fig. 5. Projection of the structure of $Gd_6Co_{1.67}Si_3$ along the *c* axis. The black and white bonds are located at the *z*-coordinate 1/4 and 3/4, respectively.

This corresponds roughly to the ratio of the number of electrons between cobalt and silicon. The structure of $Gd_6Co_{1.67}Si_3$ is close to those proposed by Prots' *et al.* for $La_6Ni_{1.54}Si_3$ and $Nd_6Ni_{1.66}Si_3$ [11, 12], the rare-earth metal and nickel atoms being replaced by gadolinium and cobalt atoms, respectively (Table 2b). The main structural difference between these three structures are the occupancy values of the Wyckoff positions 4*e* and 2*a*. In $Gd_6Co_{1.67}Si_3$ the cobalt atoms are mainly located on the 4*e* position, whereas in $La_6Ni_{1.54}Si_3$ the nickel atoms are mainly located in 2*a* position. In $Nd_6Ni_{1.66}Si_3$, the nickel atoms are well distributed over both positions with occupancy ratios of 20.3% and 25% for the 4*e* and 2*a* positions, respectively [12].

A projection of the structure along the *c* axis is displayed in Fig. 5 and the column of Co1a and Co1b positions along the *c* axis is presented in Fig. 6. The silicon atoms are located in trigonal $[Gd_6]$ prism capped by two gadolinium atoms and one cobalt atom with average Si-Gd distance of 3.07 Å in good agreement with the sum of the metallic radii ($r_{Si} = 1.319$ Å, $r_{Gd} = 1.802$ Å). The Si-Co2 distance, 2.42 Å, is slightly shorter than the sum of metallic radii ($r_{Co} = 1.252$ Å). The gadolinium atoms around the Co2 position form another trigonal $[Gd_6]$ prism with a Gd-Co distance of 2.932(5) Å. The Co1a position is shifted away from the center of an octahedron of gadolinium atoms with two different Co-Gd distances, 2.83(2) and 3.09(4) Å. The former distance seems to be short but is comparable to those observed in $Gd_{12}Co_7$, for instance [13]. The Co1b atoms are located in a trigonal prism of gadolinium atoms with Co1b-Gd1 distances of 3.449(12) Å

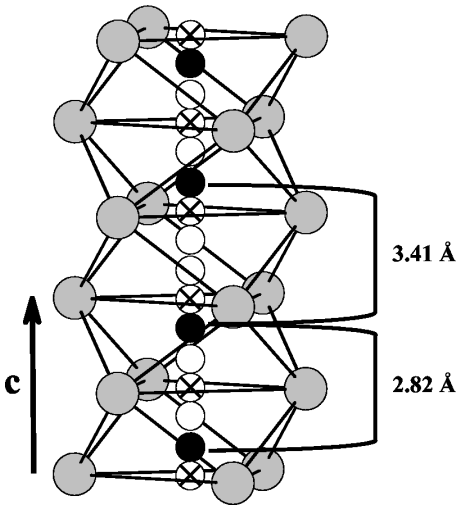

Fig. 6. View of the chain of Co1a (open and filled circles) and Co1b (circles with a cross inside) positions along the *c* axis. The open circle and filled circle have been arbitrary attributed to empty and filled Co1a positions.

and with the three rectangular faces capped by gadolinium atoms with short distances of 2.749(15) Å. This really short distance explains the very low occupancy ratio of this position by cobalt atoms. In $Gd_6Co_{1.67}Si_3$, $Nd_6Ni_{1.66}Si_3$ and $La_6Ni_{1.54}Si_3$, for cobalt or nickel atoms in the $(0,0,1/4)$ position, the relative difference between the sum of metallic radii (r_{met}) and the experimental distance (d_{exp}) *RE*-Co or *RE*-Ni ($(\Sigma r_{met} - d_{exp})/\Sigma r_{met}$) are equal to 9.7, 8.7 and 7.1%, respectively, whereas the occupancy ratios of this position are equal to 6%, 25% and 35.5%. The occupancy ratio of the $(0,0,1/4)$ position increases when the steric strain decreases. As the radius of silicon is longer than the radius of cobalt, these short Co1a-Gd and Co1b-Gd distances would be really too short for silicon atoms and thus is a supplementary argument for the transition metal distribution model. If only the most occupied position Co1a is considered, realistic Co-Co distances within the column of cobalt atoms are observed if 1/3 of the Co1a positions is filled (Fig. 6). From this simple model one can explained the non-stoichiometry of the title compound.

Two different kinds of environments are observed for gadolinium atoms. Gd1 is surrounded by 3 silicon atoms with an average distance of 3.00 Å and by 10 gadolinium atoms. The Gd-Gd distances vary from 3.449 to 4.164 Å, most of these distances being greater than the sum of the metallic radii (3.604 Å). Gd1 atoms are also surrounded by two Co1a and one Co1b positions. These positions are partially occupied and this induces a disordered surrounding for the Gd1 position. These distances are rather short, 2.749(15) and 2.83(2) Å, as previously discussed (*vide supra*). The Gd2 position is surrounded by 2 cobalt, 5 silicon and 10 gadolinium atoms. The two Gd-Co2 distances are equal to 2.932(5) Å, this distance being slightly shorter than the sum of metallic radii (3.052 Å). The Gd2-Si distances are ranging from 3.06 to 3.25 Å and thus very close to the sum of metallic radii of 3.121 Å. The Gd2-Gd2 distances are ranging from 3.576 to 4.164 Å.

Bodak *et al.* have shown that the Ce_2NiSi-, $Ce_6Ni_2Si_3$- and $Ce_{15}Ni_4Si_{13}$-type structures are closely related [14]. In their structure determinations, they have not solved the problem of the short distances between the nickel atoms on the $(0,0,z)$ positions. It is worthwhile to note that the ternary silicide $Gd_6Co_{1.67}Si_3$ belongs to the family of $Ce_6Ni_2Si_3$-type compounds. In the structure of $Ce_6Ni_2Si_3$ really short distances between nickel atoms in the $(0,0,0)$ position are observed that are not realistic (2.16 Å compared to the metallic radius $r_{Ni} = 1.246$ Å). For this compound it is clear that, as proposed by Lemaire *et al.* [10] and Prots' *et al.* [11, 12] and confirmed by the present work, the right composition should be $Ce_6Ni_{1.67}Si_3$. The same problem occurs for the Ce_2NiSi-type compounds where really short distances between nickel atoms are observed. Pecharsky *et al.* [15] have observed that in the compound $Pr_5Ni_{1.9}Si_3$ with Ce_2NiSi-type structure the Ni positions $(0,0,z)$ and $(0,0,1/4)$ cannot be fully occupied to manage realistic Ni-Ni distances.

In the sequence $Gd_6Co_{4.61}$ (or $Gd_4Co_{3.07}$) $\rightarrow$ $Gd_6Co_{1.67}Si_3$, the unit cell volume increases from 471.7 to 500.3 $Å^3$ in agreement with the replacement of cobalt by a larger silicon atom. We note also an anisotropic expansion of the unit cell parameters; the *c* parameter increases more strongly (2.7%) than the *a* parameter (1.6%). This can be explained considering that the crystal structure of $Gd_6Co_{1.67}Si_3$ (Fig. 5) is described by a stacking of trigonal prisms $[Gd_6]$ occupied by Si or Co atoms along the *c* axis. An empirically established rule [16, 17] indicates that the relative dimensions of the centered trigonal prisms $[RE_6]$ depend on the nature of the atom that occupies the center site. Thus, prisms that contain a transition metal are inclined to be compressed, while those that contain a p-block element are inclined to be stretched.

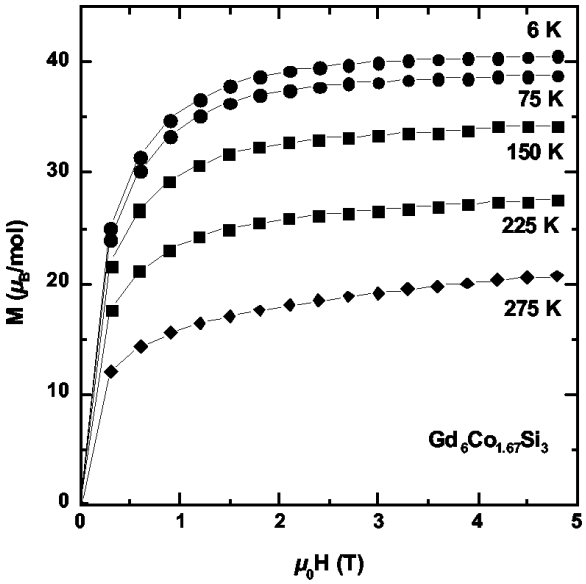

Fig. 7. Field dependence of the magnetization, measured at various temperatures, of $Gd_6Co_{1.67}Si_3$.

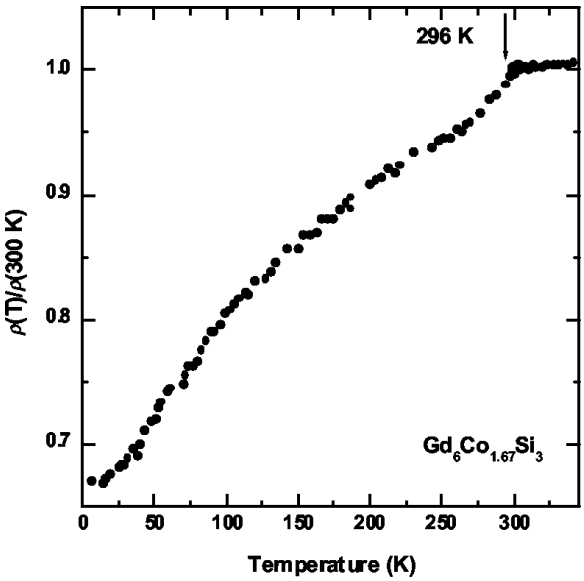

Fig. 8. Temperature dependence of the reduced electrical resistivity of $Gd_6Co_{1.67}Si_3$.

This rule turns out to be confirmed for the hexagonal compounds $Gd_6Co_{4.61}$ and $Gd_6Co_{1.67}Si_3$. One can see that the c/a ratio increases from 0.350 to 0.354 in the sequence $Gd_6Co_{4.61} \rightarrow Gd_6Co_{1.67}Si_3$ as silicon replaces the cobalt atoms, indicating the lengthening of the trigonal prisms [Gd_6]. The substitution Co-Si induces also an increase of the Gd-Gd interatomic distances; for instance Gd1-Gd1 changes from 3.40 to 3.45 Å and Gd1-Gd2 from 3.55 to 3.61 Å.

Magnetic and electrical properties

Results of magnetic measurements showing the temperature dependence and field dependence of the magnetization M of $Gd_6Co_{1.67}Si_3$ are plotted in Figs 1 and 7 respectively. The change of slope in the magnetization data M = f(T) (Fig. 1) indicates the occurrence of a ferromagnetic ordering near 294(2) K. The Curie temperature was determined from linear M^2 *vs* $\mu_0 H/M$ behaviours (Arrot plots), which is predicted by the Landau theory of second order phase transitions [18]. Isothermal magnetization performed at 6 K (Fig. 7) saturates at 5 Tesla with a saturation magnetic moment 40.7(3) μ_B/mol corresponding to 6.78 μ_B per gadolinium atom, only slightly lower than the theoretically calculated free ion Gd^{3+} value ($7\mu_B$). Also at 6 K, the hysteresis loop of the magnetization of $Gd_6Co_{1.67}Si_3$ does not show a remanence phenomenon. This characteristic agrees with the isotropic character of the Gd^{3+} ion.

The existence of a ferromagnetic transition for $Gd_6Co_{1.67}Si_3$ is confirmed by the temperature dependence of the electrical resistivity presented in Fig. 8. A sudden change of slope is detected at 296(2) K (the temperature where the derivative curve $d\rho/dT = f(T)$ exhibits a peak), in agreement with the T_C value extracted from the magnetic measurements. The decrease of ρ below T_C could be associated with the loss of spin disorder scattering of the conduction electrons owing to the appearance of a ferromagnetic transition.

It is interesting to note that the ternary silicide $Gd_6Co_{1.67}Si_3$ shows a Curie temperature similar to that reported for pure gadolinium ($T_C = 294$ K) [19]. But $Gd_6Co_{1.67}Si_3$ contains only 56% at. of Gd. Moreover the replacement of cobalt by silicon induces an increase of the Curie temperature from 220 K ($Gd_4Co_{3.07}$ or $Gd_6Co_{4.61}$) [20] to 294(2) K ($Gd_6Co_{1.67}Si_3$). This behaviour is interesting; generally, similar substitution induces a decrease of the Curie temperature. For instance, in the $Gd(Co_{1-x}Si_x)_2$ system T_C decreases weakly from 395 to 385 K when x varies from 0 to 0.20 [21]. We note that in $Gd_4Co_{3.07}$ or $Gd_6Co_{4.61}$ [20] the cobalt exhibits an induced magnetic moment of about $0.6\mu_B$/Co, which is antiparallel to the moment of Gd. Our investigation of $Gd_6Co_{1.67}Si_3$ by magnetization measurement does not

reveal a magnetic moment carried by cobalt. In order to explain the increase of T_C, the calculation of the electronic structure of $Gd_6Co_{4.61}$ and $Gd_6Co_{1.67}Si_3$ is in progress.

Conclusion

The ternary silicide $Gd_6Co_{1.67}Si_3$ is the first member of the family $RE_6Co_{1.67}Si_3$ which can be obtained for *RE* = Ce, Nd, Tb and Dy. It presents an interesting ferromagnetic ordering close to room temperature, which could be associated with a magnetocaloric effect. X-ray diffraction studies at lower and higher temperature than room temperature will be performed to observe a possible evolution of the disorder of the cobalt atoms on the $(0, 0, z)$ positions.

Acknowledgement

The authors thank L. Raison and R. Decourt for their assistance during the microprobe analysis and the electrical resistivity measurements.

[1] B. Chevalier, E. Gaudin, F. Weill, J.-L. Bobet, Intermetallics **12**, 437 (2004).
[2] B. Chevalier, S. F. Matar, Phys. Rev. B **70**, 174408 (2004).
[3] B. Chevalier, M. Pasturel, J.-L. Bobet, O. Isnard, Solid State Commun. **134**, 529 (2005).
[4] R. Welter, G. Venturini, E. Ressouche, B. Malaman, J. Alloys Compd. **210**, 279 (1994).
[5] S. A. Nikitin, T. I. Ivanova, I. G. Makhro, Yu. A. Tskhadadze, Yu. F. Popov, O. D. Chistyakov, N. F. Vadernikov, Phys. Solid State **39**, 1128 (1997).
[6] S. Wu, J. Yan, L. Zhang, W. Qin, L. Zeng, Y. Zhuang, Z. Metallkd. **91**, 373 (2000).
[7] A. V. Morozkin, S. N. Klyamkin, I. A. Sviridov, J. Alloys Compd. **316**, 236 (2001).
[8] V. Petricek, M. Dusek, The crystallographic computing system Jana2000, Institute of Physics, Praha, Czech Republic.
[9] F. Canepa, S. Cirafini, M. Napoletano, J. Alloys Compd. **335**, L1 (2002).
[10] R. Lemaire, J. Schweitzer, J. Yakinthos, Acta Crystallogr. B **25**, 710 (1969).
[11] Yu. M. Prots', W. Jeitschko, Inorg. Chem. **37**, 5431 (1998).
[12] Yu. M. Prots', W. Jeitschko, J. Solid State Chem. **137**, 302 (1998).
[13] W. Adams, J.-M. Moreau, E. Parthé, J. Schweitzer, Acta Crystallogr. B **32**, 2697 (1976).
[14] O. I. Bodak, E. I. Gladyshevskii, O. I. Kharchenko, Kristallografiya **19**, 80 (1974).
[15] A. O. Pecharsky, Yu. Mozharivskyj, K. W. Dennis, K. A. Gschneidner (Jr.), R. W. McCallum, G. J. Miller, V. K. Pecharsky, Phys. Rev. B **68**, 134452 (2003).
[16] D. Hohnke, E. Parthé, Acta Crystallogr. **20**, 572 (1966).
[17] E. Parthé, B. Chabot, E. Hovestreydt, Acta Crystallogr. B **39**, 596 (1983).
[18] K. P. Belov, Magnetic Transitions (Consultants Bureau Enterprises), New York (1961).
[19] V. K. Pecharsky, K. A. Gschneidner (Jr.), J. Magn Magn. Mater. **200**, 44 (1999).
[20] T. M. Seixas, J. M. Machado da Silva, T. P. Papageorgiou, H. F. Braun, G. Eska, Physica B **353**, 34 (2004).
[21] N. Huu Duc, J. Magn Magn. Mater. **152**, 219 (1996).